Human Brain Mapping doi: 10.1002/hbm.23505

Time course of gamma-band oscillation associated with face processing in the inferior occipital gyrus and fusiform gyrus: a combined fMRI and MEG study

Running title:
Neural basis of face processing

Author names and author affiliation:
Shota Uono,[1] Wataru Sato,[1] Takanori Kochiyama,[2] Yasutaka, Kubota,[3] Reiko Sawada,[1,4] Sayaka Yoshimura,[1] Motomi Toichi[1,4]
1 Graduate School of Medicine, Kyoto University, 53 Shogoin-Kawahara-cho, Sakyo-ku, Kyoto 606-8507, Japan.
2 ATR Brain Activity Imaging Center, 2-2-2 Hikaraidai, Seika-cho, Soraku-gun, Kyoto 619-0288, Japan.
3 Health and Medical Services Center, Shiga University, 1-1-1 Baba, Hikone, Shiga 522-0069, Japan
4 The Organization for Promoting Neurodevelopmental Disorder Research, 40 Shogoin Sannou-cho, Sakyo-ku, Kyoto 606-8392, Japan

Corresponding author:
Shota Uono, Department of Neurodevelopmental Psychiatry, Habilitation, and Rehabilitation, Graduate School of Medicine, Kyoto University, Shogoin-Kawahara-cho, Sakyo-ku, Kyoto 606-8507, Japan.
Tel: +81 75 751 3966; Fax: +81 75 751 3966; E-mail: uonoshota1982@gmail.com

Abstract

Debate continues over whether the inferior occipital gyrus (IOG) or the fusiform gyrus (FG) represents the first stage of face processing and what role these brain regions play. We investigated this issue by combining functional magnetic resonance imaging (fMRI) and magnetoencephalography (MEG) in normal adults. Participants passively observed upright and inverted faces and houses. First, we identified the IOG and FG as face-specific regions using fMRI. We applied beamforming source reconstruction and time–frequency analysis to MEG source signals to reveal the time course of gamma-band activations in these regions. The results revealed that the right IOG showed higher gamma-band activation in response to upright faces than to upright houses at 100 ms from the stimulus onset. Subsequently, the right FG showed greater gamma-band response to upright faces versus upright houses at around 170 ms. The gamma-band activation in the right IOG and right FG was larger in response to inverted faces than to upright faces at the later time window. These results suggest that 1) the gamma-band activities occurs rapidly first in the IOG and next in the FG and 2) the gamma-band activity in the right IOG at later time stages is involved in configuration processing for faces.

Keywords: Face processing; Fusiform gyrus; Gamma-band oscillation; Inferior occipital gyrus; Magnetoencephalography (MEG)

1 Introduction

The face is a fount of social information. It enables us to transmit intention and emotion through a single facial feature (e.g., the eye) [Emery, 2000] and their configurations (e.g., emotional facial expressions) [Prkachin, 2003]. Under social pressure such as cooperation and competition, adaptive mechanisms evolved to use facial information rapidly and effectively. In fact, previous studies have demonstrated that humans show more rapid detection [Purcell and Stewart, 1986] and more attentional bias towards faces [Ro et al., 2001] compared with objects, and preferentially process faces at the individual level [Tanaka, 2001].

Consistent with the behavioral significance of faces, a number of neuroimaging studies using functional magnetic resonance imaging (fMRI) and positron emission tomography have identified some specialized brain regions for face processing, such as the inferior occipital gyrus (IOG) and fusiform gyrus (FG) in the right hemisphere [Haxby et al., 2000; Yovel and Kanwisher, 2005]. Recently, two alternative views were proposed regarding the neural mechanisms for early stages of face processing. Based on the findings that the IOG sits in the intermediate position between the early visual cortex and the FG in the cortical hierarchy [Hemond et al., 2007] and that the IOG stimulation induced impairment in discriminating facial parts, but not spacing between parts [Pitcher et al., 2007], previous investigators have proposed that the IOG is an initial stage of a computational hierarchical brain network specific to face processing and represents facial parts prior to subsequent configural processing in the FG [Pitcher et al. 2011; see also Haxby et al., 2000). On the other hand, based on the finding that the FG showed specific responses to faces even in a patient with an IOG lesion [Rossion et al., 2003; Schiltz et al., 2006] and that the IOG lesion induced impairment of face individuation while preserving ability in face categorization [Steeves et al., 2006], it is thought that the FG is an early face-selective region that refines initial coarse holistic representations through interaction with the IOG, which, in turn, conducts fine-grained visual analyses [Rossion, 2008]. Debate continues over whether the IOG or the FG represents the first stage of face processing and what role these brain regions play.

Electrophysiological recordings can provide valuable information about the time course of neural activity at specific information processing stages. Several electroencephalography (EEG) studies using scalp recording to analyze event-related

potential (ERP) have shown that a first, robust face-selective ERP component was recorded at the occipitotemporal site around 170 ms after stimulus onset (N170; [e.g., Bentin et al., 1996; for a review, see Rossion and Jacques, 2008]). The source of this component was estimated to be located in the FG [Horovitz et al., 2004; Sadeh et al., 2010]. In the same time window (150–200 ms), however, intracranial EEG studies have demonstrated that the IOG showed a greater ERP to faces than to other objects [Allison et al., 1999; Jonas et al., 2012; Rosburg et al., 2010]. Based on the evidence, both the IOG and FG show stronger ERP in response to faces than to other objects at least during 150–200 ms.

The investigation of high-frequency neural activity may be a promising approach to reveal the early stage of face processing in the IOG and the FG because the face-related activity in the IOG has been consistently reported in previous fMRI studies (Liu, Harris, & Kanwisher, 2010), and hemodynamic responses reflect electrical activity in the gamma band frequency (>30 Hz) [Foucher et al., 2003]. Furthermore, gamma-band activity was related to several types of information processing [Herrmann et al., 2010], including face processing [Gao et al., 2013]. Recent magnetoencephalography (MEG) studies applied time–frequency analysis to sensor signals in response to faces, and estimated the source of gamma-band activation [Dobel et al., 2011; Gao et al., 2013]. However, the predefined time window for source estimation did not include an early stage of face processing. An additional limitation is that the estimation of neural source from MEG alone does not have a relatively high spatial resolution. Some previous intracranial EEG studies, which have relatively high spatio-temporal resolution compared with MEG, also conducted time–frequency analysis for the activity in the occipital and temporal cortices. Several studies investigated activation in the FG and found that the gamma-band activation occurred in response to faces at around 170 ms and later [Engell and McCarthy, 2011; Klopp et al., 1999; Lachaux et al., 2005]. A recent study investigated IOG activity [Sato et al., 2014] and reported that the IOG showed a stronger gamma-band activity in response to faces than to houses or mosaics at about 100 ms after stimulus onset. Collectively, these intracranial EEG data suggest that the gamma-band activation could be shown first in the IOG and then in the FG during face processing. However, there has been no intracranial EEG study that compared gamma-band activity in the IOG and the FG because the location of electrode

implantation was determined solely by clinical necessity. Furthermore, it might be possible that clinical conditions in participants, such as epileptic seizures, affect neural activity in the recorded regions. Thus, the temporal features of gamma-band activities in the IOG and FG remain inconclusive. We aimed to investigate face-specific neural activities of the IOG and the FG using a method with high spatio-temporal resolution in healthy participants. Based on the above-mentioned findings, we hypothesized that a face-specific gamma-band activation of the IOG precedes that of the FG.

As mentioned above, debate also persists regarding whether the IOG and the FG are involved in featural or configural processing at the early processing stage. Behavioral studies have found that the presentation of inverted faces compromises the processing of configural information [Maurer et al., 2002]. Based on this, differential activation in response to upright and inverted faces has been interpreted as playing a role in configural processing. Previous intracranial EEG studies found that, compared with upright faces, inverted faces elicited higher-amplitude ERP around 200 ms in the IOG [Rosburg et al., 2010] and the FG [Pourtois et al., 2010]. These studies suggest that low-frequency band activity in the IOG and the FG are associated with configural processing. Although a previous study demonstrated greater gamma-band activity in the IOG in response to upright than to inverted faces at around 200 ms [Sato et al., 2014], no study has investigated gamma-band response in the FG at an early time window. Based on the finding suggesting that the IOG and FG contribute to the processing of facial configuration, we hypothesized that gamma-band oscillation in both regions discriminates between upright and inverted faces.

The present study aimed to investigate whether the IOG or the FG represents the first stage of face processing and how these brain regions contribute to feature and configural processing. We investigated this issue by recording fMRI and MEG in normal participants, which allowed us to obtain both spatial and temporal information on gamma-band activations. Photographs of upright and inverted faces and houses were presented, and participants passively viewed the stimuli during a dummy target-detection task. We localized the regions in the bilateral IOG and FG that are involved in face processing using fMRI signals. We then analyzed MEG signals in these regions using beamforming source reconstruction and time–frequency analysis. Based on previous intracranial EEG findings [e.g., Engell and McCarthy, 2011; Sato et al., 2014],

we predicted that the face-specific gamma-band activation in the IOG would occur at around 100 ms after stimulus onset and would be followed by the FG activation, particularly in the right hemisphere. Also, based on some previous data [Pourtois et al., 2010; Sato et al., 2014], we predicted that upright and inverted faces would show different activation patterns in the gamma-band, as well as in the low-frequency bands, in the IOG and FG at relatively later time windows.

2 Material and Methods

2.1 Participants

Thirty-three volunteers underwent fMRI and MEG recordings (17 males; mean ± standard deviation [*SD*]: age, 22.06 ± 3.58 years). All participants were right-handed, as assessed by the Edinburgh Handedness Inventory [Oldfield, 1971], and had normal or corrected-to-normal visual acuity. All participants provided written informed consent, which was approved by the ethics committee of the Primate Research Institute, Kyoto University. The experiment was conducted in accordance with the Declaration of Helsinki.

2.2 Design

The experiment was conducted using a within-participant two-factorial design with stimulus type (face or house) and orientation (upright or inverted) as the factors.

2.3 Stimuli

The face and house stimuli (Fig. 1) were selected from those used in a previous study [Sato et al., 2014]. Face photographs with neutral expressions of five female and five male Japanese models were used as face stimuli. The stimuli subtended a visual angle of 10.0° vertical × 10.0° horizontal. The house stimuli consisted of photographs of 10 houses and were the same size as the face stimuli. For the inverted condition, all face and house photographs were turned upside down. All stimuli were depicted in grayscale. The mean luminance of each stimulus was held constant using MATLAB 6.5 (Mathworks).

2.4 Apparatus

Experimental events were controlled by Presentation software (version 10.0; Neurobehavioral System), which was implemented on a Windows computer. The stimuli were projected to a mirror positioned in front of the subjects using a liquid crystal projector (fMRI: DLA-HD10KHK, Victor; MEG: DLA-G150CL, Victor).

2.5 Procedures

For both fMRI and MEG recordings, during each trial, a black fixation cross (visual angle: 1.0° vertical × 1.0° horizontal) was presented at the center of the screen for 1,000 ms. Then, a face or house stimulus appeared for 500 ms. As target trials, instead of the face and house stimuli, a red cross (visual angle: 1.4° vertical × 1.4° horizontal) replaced the fixation cross. Participants were asked to detect the red fixation cross and to press a button with the right forefinger as quickly as possible. These dummy tasks confirmed that participants were attending to the stimuli but did not require controlled cognitive, emotional, or behavioral processing of the stimuli. Performance on the dummy target-detection task was good (mean ± *SD* detection rate = 96.24 ± 10.28 and 96.39 ± 7.45 %; mean ± *SD* reaction times: 529.36 ± 99.89 and 455.92 ± 70.30 ms for fMRI and MEG studies, respectively).

For the fMRI recording, the inter-trial interval was fixed at 1,500 ms, and a block design was used. The scan session consisted of 16 epochs of 24 s each, interspersed with 16 rest periods, each 24 s long (a blank screen). In total, the task consisted of 128 trials (30 trials each for the upright face, upright house, inverted face, and inverted house stimuli, plus eight target trials). Each condition was presented in different epochs within each scan. The order of epochs within each scan was pseudo-randomized, and the order of stimuli within each epoch was randomized. To familiarize participants with the procedure, 16 practice trials preceded the experiment.

In the MEG recording, participants were additionally instructed not to blink during the presentation of stimuli. The inter-trial interval varied randomly between 800 and 1,000 ms. The task consisted of 360 trials (80 trials each for the upright face, upright house, inverted face, and inverted house stimuli, plus 40 target trials). These trials were divided into 10 blocks and were presented in pseudo-random order. Participants were allowed to rest between blocks to avoid habituation and drowsiness. To familiarize participants with the procedure, 36 practice trials preceded the experiment.

2.6 MRI acquisition

Image scanning was performed on a 3-T scanning system at the ATR Brain Activity Imaging Center (MAGNETOM Trio, A Tim System, Siemens) using a 12-channel array coil. The functional images consisted of 40 consecutive slices parallel to

the anterior–posterior commissure plane covering the whole brain. A T2*-weighted gradient-echo echo planar imaging sequence was used with the following parameters: repetition time (TR) = 2,500 ms; echo time (TE) = 30 ms; flip angle (FA) = 80°; field of view (FOV) = 192 ×192 mm; matrix size = 64 × 64; voxel size = 3 × 3 × 4 mm, without acceleration mode. The order of slices was ascending. Elastic pads placed on all sides of the participant's head were used to stabilize head position during functional image acquisition.

After the acquisition of functional images, a T1-weighted high-resolution anatomical image was also obtained using a magnetization-prepared rapid gradient-echo sequence (TR = 2,250 ms; TE = 3.06 ms; FA = 9°; inversion time = 1,000 ms; FOV = 256 × 256 mm; matrix size = 256 x 256; voxel size = 1 × 1 × 1 mm).

2.7 MEG acquisition

MEG acquisition was performed in an electromagnetically shielded room using a 400-channel whole-head supine-position system (PQ1400RM; Yokogawa). A forehead strap was used to stabilize head position. MEG data were sampled at 1,000 Hz through a band-pass of 0.05–200 Hz. Vertical and horizontal electrooculograms (EOGs) were simultaneously recorded.

To measure head position within the MEG sensor system, five small coils were mounted on the participants' heads. An electromagnetic calibration of the coil positions was performed before and after each MEG recording session. Participants' head shape and calibration coil positions were digitized with a three-dimensional (3D) laser-optical scanner and a stylus marker (FastSCAN Cobra; Polhemus) and were later used to co-register the MEG sensor locations to an anatomical space defined by an individual MRI.

2.8 Data analysis: fMRI

Data analyses both for fMRI and MEG were performed using the statistical parametric mapping package SPM8 (http://www.fil.ion.ucl.ac.uk/spm).

For fMRI, images of each run were realigned with the first scan as a reference to correct for head movements. Data from all subjects showed a small motion correction (~2 mm). The T1 anatomical image was preprocessed by intensity inhomogeneity correction. Then, T1 anatomical images were coregistered to the first scan of the functional images. Following this, the coregistered T1 anatomical image was normalized to Montreal Neurological Institute space using the unified segmentation–

spatial normalization approach [Ashburner and Friston, 2005]. The parameters from this normalization process were then applied to each of the functional images. Finally, these spatially normalized functional images were resampled to a voxel size of 2 × 2 × 2 and smoothed with an isotopic Gaussian kernel of 8 mm at full-width at half-maximum to compensate for anatomical variability among participants.

Significantly activated voxels were searched using random-effects analysis. First, single-subject analyses were performed [Friston et al., 1995]. The design matrix contained four task-related regressors (upright face, inverted faces, upright houses, and inverted houses) and one target-related regressor, which were convolved with a canonical hemodynamic response function (HRF). To eliminate an artifact of low frequency trend, the high-pass filter, composed of the discrete cosine basis function with a cut-off period of 128, was used. To reduce the motion-related artifacts, the six realignment parameters of the rigid-body transformation were added to the model. Serial autocorrelation, assuming a first-order autoregressive model, was estimated from the pooled active voxels using a restricted maximum likelihood (ReML) procedure and was used to whiten the data and design matrix [Friston et al., 2002]. The least-square estimation was performed on the high-pass-filtered and pre-whitened data and design matrix. The weighted sum of the parameter estimates in the single-subject analysis constituted contrast images that were used for the second level analysis.

A random-effects model analysis was conducted to make statistical inferences at the population level [Holmes and Friston, 1998]. The contrast images of upright face, inverted face, upright house, and inverted house vs. rest for each participant were entered into the flexible factorial model in SPM, generating a two-way repeated-measures analysis of variance (ANOVA) to create a random-effect SPM{*T*}. The model included stimulus type and orientation as factors of interest; participant was a factor of no interest. Then, planned comparisons between faces and houses were performed. Significantly activated clusters were identified if they reached a height threshold of $p < 0.05$ (familywise-error-corrected). The results revealed that the bilateral IOG and FG were activated in response to faces versus houses.

2.9 Data analysis: MEG

Continuous MEG data were epoched into 900-ms segments for each trial and down-sampled to 200 Hz; pre-stimulus baseline data were collected for 300 ms, and

experimental data were collected for 600 ms after stimulus onset. The data were initially subjected to independent component analyses (ICA) for the purpose of artifact rejection using EEGLAB toolbox (http://sccn.ucsd.edu/eeglab/index.html). The ICA components (ICs) were visually inspected, and those representing eye artifacts, heartbeat, or muscle activity were rejected. The rest of the ICs were projected back to the MEG sensor space to obtain a "clean" MEG signal. Threshold-based artifact rejection was also conducted. Any epochs containing a gradiometer amplitude ≥3,000 fT/cm and an EOG amplitude ≥ ± 80 μV were rejected as artifacts. One participant was excluded from further analysis because an extremely high proportion of trials were contaminated by various artifacts. Among the remaining participants, the number of trials without artifact contamination did not differ across conditions (mean ± *SD* = 63.49 ± 8.48; F (1, 31) = 2.32, $p > 0.05$). The pre-processed data were baseline corrected based on the 300-ms pre-stimulus period.

For the beamformer analyses, first, the cortical mesh on which the current dipoles were placed was created. The individual anatomical MRI of each participant was segmented and spatially normalized to the MNI space. The inverse of this normalization transformation was then used to warp a canonical cortical mesh in the MNI space to the individual cortical mesh [Mattout et al., 2007]. The cortical mesh described the source locations with 20,484 vertices (i.e., "fine" size). Next, the MEG sensors were co-registered to anatomical MRI data by matching the positions of three fiducials (nasion and R- and L-preauricular points) and head shape. The forward model could then be computed using a "single sphere" model by assuming that the orientations of the sources were normal to the cortical mesh.

Based on the forward model, the Linearly Constrained Maximal Variance (LCMV) beamformer as a part of the SPM8 was used to transform the original sensor time series data into source-space time-series data [van Veen et al., 1997]. We identified face-specific ROIs in each participant using an fMRI contrast between responses to upright faces versus houses. The peak foci (height threshold, $p < 0.01$) in 8-mm radius spheres centered on the average peak coordinates of the bilateral IOG and FG were used for the time–frequency analysis. In cases where no peak foci appeared in the spheres, the average peak coordinates across participants were used. MEG source signals within 8-mm radius spheres centered on the identified coordinates were extracted by LCMV

beamformer with 0.01% regularization.

To calculate the time–frequency maps for each trial, a seven-cycle morlet wavelet time–frequency analysis ranging from 4 to 100 Hz with a frequency resolution of 1 Hz was applied to the source activity in each ROI. Data were then log transformed and baseline corrected (-200 to 0 ms), and a weighted average of time–frequency trials was calculated within participants by condition. The time–frequency maps were converted into 2D images. Based on the findings of previous intracranial EEG studies investigating face-specific gamma-band activity [e.g., Parvizi et al., 2012; Sato et al., 2014], the time window of interest for face processing was restricted to 100–400 ms after stimulus onset using explicit masking. This time window is also congruent with a theoretical suggestion that the cortical activation in response to visual stimuli starts at around 100 ms (e.g., 96 ms [David et al., 2006]). The time–frequency maps (100–400 ms and 4–100 Hz) were entered into a within-subject ANOVA including upright faces, upright houses, inverted faces, and inverted houses as factors.

Statistical inferences performed on the time–frequency SPM {*T*} data were based on random field theory [Kilner et al., 2005; Worsley et al., 1996]. According to our interests, the contrasts between upright faces and upright houses, between upright faces and inverted faces, and between inverted faces and upright faces were tested for each ROI. The data reflected inconclusive results across studies using different measurements with respect to whether upright or inverted faces elicited greater activity in the occipitotemporal cortex [e.g., Meeren et al., 2008; Sato et al., 2014]. A previous intracranial study also found that the contrasts between inverted and upright faces and between upright and inverted faces elicited significant activation at the gamma and low-frequency bands, respectively [Sato et al., 2014]. Thus, we analyzed the contrasts between upright and inverted faces and between inverted and upright faces independently. Significantly activated time-frequency clusters were identified if they reached a height threshold of $p < 0.05$ (uncorrected) with an extent threshold of $p < 0.05$ familywise-error-corrected for multiple comparisons over the whole time–frequency space (100–400 ms and 4–100 Hz; total voxels = 5,917). The equivalent *Z* value was used to report the statistical inferences. Because the temporal resolution of low-frequency activity is generally poor in time–frequency analyses, the latencies are only discussed for gamma-band activity.

A time–frequency analysis on evoked responses was performed first to ensure that the early face-specific gamma oscillations identified in the analyses did not reflect only evoked responses to faces (e.g., N170). Time–frequency maps of the averaged data across trials were calculated for each condition. The evoked responses to upright faces were stronger than those to houses in the right IOG (140–280 ms, 23–38 Hz: $Z = 3.27$) and right FG (250–400 ms, 22–32 Hz: Z = 4.11) (height threshold of $p < 0.05$, uncorrected, with an extent threshold at $p < 0.05$ familywise-error-corrected for multiple comparisons). Although the evoked responses may contribute to face-specific activations at a low-frequency band, specifically in the right FG, the time–frequency profiles of these clusters did not match those of face-specific gamma oscillations (see Supplementary Figures 1 and 2).

An additional preliminary analysis was conducted to investigate whether the results of the time–frequency analysis reflected source activity in the fMRI-constrained ROIs. The forward model was inverted using a parametric empirical Bayesian framework [Mattout et al., 2007] with optimization of multiple sparse priors using a greedy search algorithm [Friston et al., 2008]. Based on the MEG results, 3D source-reconstructed images in the MNI standard space of induced activity (4–100 Hz) were obtained between 100 and 300 ms in the post-stimulus window. The source-reconstructed images were entered into a within-subject ANOVA including upright faces, upright houses, inverted faces, and inverted houses as factors. The contrasts of the upright faces versus houses revealed significant activation in the 8-mm radius spheres centered on the fMRI peak coordinates in the bilateral IOG and FG ($p < 0.05$, see Supplementary Figure 3). No significant activations were observed in adjacent regions. These findings suggest that the time–frequency analysis reflected the source activity within fMRI-constrained ROIs.

3 Results

3.1 fMRI

To identify regions showing a face-specific response, the contrast of upright faces versus upright houses was investigated (Fig. 2). The group analysis revealed a significant cluster covering the visual cortices in the right hemisphere including the activation foci in the IOG (x 54, y -76, z -4, $T = 6.70$) and FG (x 42, y -48, z -20, $T =$

8.99) and two significant clusters in the left hemisphere (IOG: x -40, y -80, z -8, T = 6.58; FG: x -42, y -52, z -18, T = 7.30). No other significant area of activation was detected with our predefined thresholds.

3.2 MEG

3.2.1 Gamma-band activity (30–100 Hz)

The estimated source activities in bilateral IOG and FG were subjected to the time–frequency analysis. The time–frequency maps in each condition and significant clusters in each contrast are shown in Figures 3 and 4, respectively.

For the contrast of upright face versus upright houses, the first significant gamma-band activation was found in the right IOG (100–160 ms, 34–49 Hz, Z = 3.34), which was followed by significant activation in the right FG (124–215 ms, 30–48 Hz, Z = 3.50; Figure 5). After 200 ms, significant high-frequency gamma activity was observed in the right IOG (200–254 ms, 60–80 Hz, Z = 3.00) and right FG (200–245 ms, 71–100 Hz, Z = 3.28; 285–320 ms, 79–100 Hz, Z = 4.05). The left FG showed greater gamma-band activity in response to upright faces than to upright houses in a later time window (325–390 ms, 44–59 Hz, Z = 3.45). There was no significant cluster in other time regions and other brain regions. To confirm the temporal differences across the face-specific gamma-band activities in the right IOG and FG, we conducted a window-of-interest analysis. The averaged power in 100–120-ms intervals and 34–49-Hz frequencies, which showed significant differences across frequencies in the right IOG, were extracted and entered into a repeated measures ANOVA with ROI (IOG and FG) and stimulus (upright faces and upright houses) as factors. The interaction between ROI and stimulus was significant ($F(1,31) = 5.11$, $p = 0.03$), indicating that the gamma oscillation in response to faces was greater than that in response to houses in the right IOG ($t(31) = 2.97$, $p = 0.006$) but not in the right FG ($t(31) = 0.39$, $p = 0.7$). These findings suggest that the right IOG shows the first face-specific gamma-band activity.

For the contrast of inverted versus upright faces, gamma-band activation was significant in the right FG (236–320 ms, 36–46 Hz, Z = 3.13) and the right IOG (295–385 ms, 25–43 Hz, Z = 2.62). No significant activation was found in any other time or brain regions.

The contrast of upright versus inverted faces did not show any significant activation at any time or in any brain region.

3.2.2 Low-frequency band (4–30 Hz)

For the contrast of upright faces versus upright houses, all ROIs revealed significant activations. In the right IOG, a significant cluster was found at the theta–alpha band (100–295 ms, 4–13 Hz, $Z = 3.34$). In the right FG, two significant clusters were shown across frequency bands (theta–alpha: 100–400 ms, 4–14 Hz, $Z = 3.10$; beta: 110–324 ms, 15–29 Hz, $Z = 4.09$). In the left IOG, a significant cluster was found around the beta band (100–350 ms, 9–21 Hz, $Z = 3.85$). In the left FG, two significant clusters also appeared across frequency bands (100–364 ms, 6–21 Hz, Z = 3.23; 145–235 ms, 21–34 Hz, Z = 2.74).

For the contrast of inverted versus upright faces, the right IOG showed significant clusters across frequency bands (theta: 100–400 ms, 4–7 Hz, $Z = 3.44$; alpha–gamma: 100–400 ms, 8–34 Hz, $Z = 4.15$). In the left IOG, a significant cluster spread across the theta and alpha bands (100–390 ms, 4–15 Hz, $Z = 3.51$).

The contrast of upright versus inverted faces did not show significant activation at any time in any brain region.

4 Discussion

Our results of the fMRI experiment revealed that face stimuli induced enhanced activation in the bilateral IOG and FG compared with house stimuli. These results are consistent with the growing body of fMRI literature that identified the IOG and the FG as face-specific regions [Haxby et al., 2000; Yovel and Kanwisher, 2005].

More importantly, our results of MEG time–frequency analysis revealed the temporal dynamics of face selective gamma-band activation in the right IOG and FG. The gamma-band activation in the right IOG was greater for upright faces than for houses as early as 100 ms. The right IOG activation was followed by the right FG activation in response to upright faces. These results are consistent with two lines of previous electrophysiological evidence. First, a recent intracranial recording study reported greater gamma-band activation (>36Hz) in response to upright faces versus houses at around 100 ms after stimulus onset in the right IOG [Sato et al., 2014]. Second, other intracranial EEG studies have observed more FG activation to faces at around 170 ms and later time windows [Engell and McCarthy, 2011; Gao et al., 2013; Klopp et al., 1999; Lachaux et al., 2005]. However, to date, no study has directly

recorded and compared the activities in the IOG and FG during face processing and all of these studies tested clinical samples. The present data show that the gamma-band activity of the right IOG but not the right FG differed in response to upright faces and houses at 100-120 ms, suggesting that the right IOG demonstrates the first face-specific gamma-band activity. To our knowledge, this is the first direct comparisons of the activation of the IOG and the FG in normal young adults and indicates that the gamma-band activities rapidly occur first in the IOG and next in the FG at early stages of face processing.

Comparing the gamma-band activation between the presentation of upright and inverted faces would provide a clue to infer the functional role of the right IOG at the early processing stage. The results showed that there was no difference in the right IOG gamma-band activation between the presentation of upright and inverted faces until about 300 ms after stimulus onset. Our previous study also demonstrated that gamma-band activation in the right IOG at the early time window was greater both for upright and inverted faces as compared with other objects and that the activation did not differ between upright and inverted faces [Sato et al., 2014]. This suggests that the gamma-band activation in the right IOG at an early time window would be involved in the processing of facial information which is not likely to be influenced by typical facial configuration. This interpretation is also consistent with a hierarchical view that the IOG represents facial parts prior to subsequent configural processing in the FG [Pitcher et al, 2011]. Previous fMRI and TMS studies have suggested that the IOG plays an important role for processing facial parts [Liu et al., 2010] at an early processing stage around 100 ms [Pitcher et al., 2007]. Collectively, these data suggest that the right IOG might be the seat of an initial stage of face processing representing facial parts information.

Gamma-band activation in the right IOG was stronger in response to inverted than to upright faces 295–385 ms after stimulus onset. The result is consistent with the finding from an intracranial study demonstrating differential gamma-band activation of the right IOG to upright and inverted faces after 200 ms [Sato et al., 2014]. Given that the inversion of faces disrupts the processing of configural information [Maurer et al., 2002], the difference in gamma-band activation between inverted and upright faces suggests that configural processing is more demanding during the observation of

inverted than upright faces. Several lesion [Rossion et al., 2003] and stimulation [Jonas et al., 2012; 2014] studies have also demonstrated that the right IOG is necessary for the configural processing and the recognition of facial identity. Furthermore, a recent fMRI study suggested that the IOG activity had sensitivity to both facial parts and configuration [Zhao et al., 2014]. Together with these data, the present findings suggest that the gamma-band activity in the right IOG is also involved in the configural processing.

After 200 ms, face-specific gamma-band activations of the right IOG and the FG occurred in the same time window. Rossion [2008] proposed that the crude holistic representation of the face is refined through an interaction with the IOG, which allows fine-grained visual analysis. Consistent with this theory, a recent electrical stimulation study reported that stimulation of the right FG induced subjective perceptual distortions of face identity [Parvizi et al., 2012]. Stimulation of the right IOG induced subjective difficulty in perceiving spatial relationships between facial features and integrating parts as a whole [Jonas et al., 2012]. Previous fMRI studies also showed that the FG activity was correlated with a success for conscious perception of faces [Tong et al., 1998]. Although gamma-band activity did not discriminate between upright and inverted faces around 200 ms, activity in the low-frequency band was greater in response to inverted than to upright faces in the right IOG; the peak activity occurred around 220 ms, suggesting that configural processing started around this time window. Based on these findings, we speculate that the temporal coincidence of gamma-band activity in both regions reflects the interaction that mediates refinement of the holistic representation through fine-grained visual analysis, resulting in conscious perception of each face. Greater gamma-band activity in response to inverted versus upright faces in the right IOG and FG temporarily overlapped around 300 ms. The delay in processing inverted compared with upright faces suggests that processing the integrating parts of inverted faces as a whole is more demanding because inversion disrupts the processing of configural information.

An accurate understanding of the spatio-temporal pattern of activation in the IOG and FG would be valuable for building an early-stage face processing model. Pitcher et al., [2011] proposed that the IOG is an initial stage of face processing and represents facial parts prior to subsequent configural processing in the FG whereas others argued

that the FG is a first face-selective region and that the initial coarse holistic representation is then refined through the interaction with the IOG [Rossion, 2008]. Based on the interpretation described above, the results of the current study suggest an eclectic model merging these propositions; the right IOG activation at around 100 ms after stimulus onset represents the first face-specific processing, and this region is involved not only in the processing of facial parts but also in configuration at a later time window. Given the existence of reciprocal structural and functional connectivity between the IOG and the FG [Ewbank et al., 2013; Pyles et al., 2013], the activation of the right FG in parallel with that of the right IOG might reflect the formation of fine visual representation of faces through the interaction with the IOG. However, lesion studies challenge the idea that the FG is activated by an input from the IOG. For example, even after an IOG lesion, the FG showed face-specific response [Rossion et al., 2003; Schiltz et al., 2006], and the ability to categorize faces was preserved [Steeves et al., 2006]. Although the current data did not show that face stimuli induce larger gamma-band activation in the right FG than house stimuli did at early time window (100 ms), gamma-band activation to faces in the right FG was visually inspected (Figure 3). This suggests the possibility that the primary visual cortex also sends inputs to the FG, bypassing the IOG. Further studies using dynamic causal modeling for electrophysiological data are needed to investigate the time course of the interactive relationship between these regions during face processing.

It should be noted that face-specific responses were recorded at two distinct gamma-band frequency ranges. Whereas face-specific activity in the lower gamma-band range (30–50 Hz) was observed in the right IOG and FG before 200 ms, activation in the higher range (60–100 Hz) occurred after 200 ms. Our findings are consistent with those of a previous intracranial study that found face-specific activity in the right IOG occurred first in the low gamma-band range and was subsequently extended to the high range [Sato et al., 2014]. Several MEG and intracranial studies of face processing have reported peak gamma-band activity in the high frequency (>50 Hz) range around 200–300 ms [Davidesco et al., 2013; Grutzner et al., 2013; Perry & Singh, 2014; Tsuchiya et al., 2008, Vidal et al., 2010]. Previous findings suggest that gamma-band activity in the 30–60 Hz and >60 Hz ranges are differentially modulated by various stimulus properties and cognitive manipulations, suggesting that these frequency bands have

distinct functional roles in cognitive processing [Uhlhaas et al., 2011]. Furthermore, our finding that the low and high gamma-band responses occurred in different time windows suggests that the activity was involved in different aspects of face processing. However, the functional role of gamma-band activation at these frequencies remains unknown. Further studies are needed to investigate the various factors that modulate face processing at gamma-band frequencies of 30–60 Hz and above 60 Hz.

Hemispheric differences in gamma-band activation in response to faces should be also noted. In contrast to the gamma-band activation of the right hemisphere, there was no face-specific gamma-band activation in the left IOG and FG at an early time window (see Fig. 3), through the significant cluster for the contrast of upright faces versus houses at low frequency band extended to gamma-band. The results are consistent with previous electrophysiological studies showing the right hemispheric lateralization of gamma-band activation to faces [Gao et al., 2013; Sato et al., 2014]. The hemispheric lateralization in the early time window suggests that gamma-band activation in the right hemisphere plays a crucial role for detecting and recognizing other's faces. However, the left FG showed stronger gamma-band activation in response to upright faces than to houses around 350 ms. Further, the IOG in the left hemisphere showed the face inversion effect at a low frequency band, suggesting the involvement in the configural processing. Further studies are needed to investigate whether right and left hemisphere realize specific functional roles for face processing.

There are some methodological limitations of the current study as listed below. First, the task used in the current study was a passive viewing of upright and inverted faces and houses. Although previous behavioral studies showed that the inverted presentation of faces impairs configural processing of faces [Maurer et al., 2002], it is pointed out that the inversion also has an influence on the processing of facial parts [Doi et al., 2007; Rakover, 2012]. To determine functional roles of the IOG and the FG during an early stage of face processing, it would be favorable to manipulate facial parts and configuration separately [Liu et al., 2010] or to demand the processing of each aspect. Second, we investigated the estimated electrical source activity in face processing regions (the IOG and the FG) defined by an fMRI experiment. However, other brain regions may be involved in early-stage face processing. Previous studies have proposed that the amygdala rapidly processes facial information and

subsequently modulates cortical activities [Sato et al., 2013]. Previous MEG studies have reported early enhanced activity (around 100 ms) in response to inverted faces relative to upright faces, although the activity was located primarily in the medial occipital cortex which is involved in low-level visual processing rather than in the lateral occipitotemporal cortex, which is associated with face processing [Linkenkaer-Hansen et al., 1998; Meeren et al., 2008]. Further MEG and intracranial recording studies are needed to investigate the relationship between cortical and subcortical regions. Third, we did not control for the spatial frequency characteristics in the stimulus categories. A previous study showed that event-related activity in the middle occipital region (V1/V2) around 100 ms post-stimulus onset was more sensitive to noise spatial frequency than to face visibility, whereas activity in the occipitotemporal region around 170 ms post-stimulus onset was related to face visibility [Tanskanen et al., 2005]. We found face-specific gamma-band activity in the lateral occipitotemporal region but not in the middle occipital region, suggesting that the gamma-band activity was not sensitive to the spatial frequency characteristics of the stimuli. However, to exclude a potential effect of spatial frequency on early gamma-band activation in response to faces, further studies using control stimuli with spatial frequency characteristics similar to faces are needed.

5 Conclusions

Using MEG combined with fMRI, the current study investigated time courses for gamma-band activation (30–100 Hz) of bilateral IOG and FG in response to upright and inverted faces and houses. The results of the time–frequency analysis showed that the right IOG is first activated in response to upright faces versus houses at around 100 ms after stimulus onset. Subsequently, compared with houses, upright faces induce greater gamma-band response in the right FG at around 170 ms. This suggests that the right IOG is the initial stage of face processing and the right FG receives input from the results of IOG computation. Further, in parallel with the right FG activation, gamma-band activation of the right IOG is larger in response to upright faces than to houses after 200 ms, suggesting an interaction between the right IOG and right FG. The finding that low-frequency band activity was greater in response to inverted relative to upright faces in the right IOG around this time window, suggests that configural processing

starts at 200 ms. Thus, we speculate that the temporal coincidence of gamma-band activation in response to upright and inverted faces may reflect an interaction that mediates the refinement of the crude representation of the face through fine-grained visual analysis, resulting in conscious perception of each face. These results could encourage consideration of an eclectic idea between hierarchical and recurrent face processing models.

Funding

This study was supported by a Grant-in-Aid for JSPS Fellows (11J05000 to SU), the JSPS Funding Program for Next Generation World-Leading Researchers (LZ008 to WS), and the Organization for Promoting Neurodevelopmental Disorder Research. The funding sources had no involvement in study design; in the collection, analysis, and interpretation of data; in the writing of the report; and in the decision to submit the article for publication. The authors have no conflict of interest to declare.

Acknowledgements

We thank ATR Brain Activity Imaging Center for their support in acquiring the data.

References

Allison T, Puce A, Spencer DD, McCarthy G (1999): Electrophysiological studies of human face perception. I: potentials generated in occipitotemporal cortex by face and non-face stimuli. Cereb Cortex 9:415–430.

Ashburner J, Friston KJ (2005): Unified segmentation. Neuroimage 26:839–851.

Bentin S, Allison T, Puce A, Perez E, McCarthy G (1996): Electrophysiological studies of face perception in humans. J Cogn Neurosci 8:551–565.

David O, Kiebel SJ, Harrison LM, Mattout J, Kilner JM, Friston KJ. (2006): Dynamic causal modeling of evoked responses in EEG and MEG. Neuroimage. 30:1255–1272.

Davidesco I, Zion-Golumbic E, Bickel S, Harel M, Groppe DM, Keller CJ, Schevon CA, McKhann GM, Goodman RR, Goelman G, Schroeder CE, Mehta AD, Malach R (2014): Exemplar selectivity reflects perceptual similarities in the human fusiform cortex. Cereb Cortex 24:1879–1893.

Dobel C, Junghöfer M, Gruber T (2011): The role of gamma-band activity in the representation of faces: reduced activity in the fusiform face area in congenital prosopagnosia. PLoS One 6:e19550.

Doi H, Sawada R, Masataka N (2007): The effects of eye and face inversion on the early stages of gaze direction perception—An ERP study. Brain Res 1183:83-90.

Emery NJ (2000): The eyes have it: the neuroethology, function and evolution of social gaze. Neurosci Biobehav Rev 24:581–604.

Engell AD, McCarthy G (2011): The relationship of gamma oscillations and face-specific ERPs recorded subdurally from occipitotemporal cortex. Cereb Cortex 21:1213–1221

Ewbank MP, Henson RN, Rowe JB, Stoyanova RS, Calder AJ (2013): Different neural mechanisms within occipitotemporal cortex underlie repetition suppression across same and different-size faces. Cereb Cortex 23:1073–1084.

Foucher JR, Otzenberger H, Gounot D (2003): The BOLD response and the gamma oscillations respond differently than evoked potentials: an interleaved EEG-fMRI study. BMC Neurosci 4:22.

Friston K, Chu C, Mourão-Miranda J, Hulme O, Rees G, Penny W, Ashburner J (2008): Bayesian decoding of brain images. Neuroimage 39:181–205.

Friston KJ, Holmes AP, Poline JB, Grasby PJ, Williams SC, Frackowiak RSJ, Turner R (1995): Analysis of fMRI time-series revisited. Neuroimage 2:45–53.

Friston KJ, Penny W, Phillips C, Kiebel S, Hinton G, Ashburner, J (2002): Classical and Bayesian inference in neuroimaging: theory. Neuroimage 16:465–483.

Gao Z, Goldstein A, Harpaz Y, Hansel M, Zion-Golumbic E, Bentin S (2013): A magnetoencephalographic study of face processing: M170, gamma-band oscillations and source localization. Hum Brain Mapp 34:1783–1795.

Grützner C, Wibral M, Sun L, Rivolta D, Singer W, Maurer K, Uhlhaas PJ (2013): Deficits in high- (>60 Hz) gamma-band oscillations during visual processing in schizophrenia. Front Hum Neurosci 7:88.

Haxby JV, Hoffman EA, Gobbini MI (2000): The distributed human neural system for face perception. Trends Cogn Sci 4: 223–232.

Hemond CC, Kanwisher NG, Op de Beeck HP (2007): A preference for contralateral

stimuli in human object- and face-selective cortex. PLoS One 2:e574.
Herrmann CS, Frund I, Lenz D (2010): Human gamma-band activity: a review on cognitive and behavioral correlates and network models. Neurosci Biobehav Rev 34:981–992.
Holmes AP, Friston KJ (1998): Generalizability, random effects and population inference. Neuroimage 7:S754.
Horovitz SG, Rossion B, Skudlarski P, Gore JC (2004): Parametric design and correlational analyses help integrating fMRI and electrophysiological data during face processing. Neuroimage 22:1587–1595.
Jonas J, Descoins M, Koessler L, Colnat-Coulbois S, Sauvée M, Guye M, Vignal J-P, Vespignani H, Rossion B, Maillard L (2012): Focal electrical intracerebral stimulation of a face-sensitive area causes transient prosopagnosia. Neurosci 222:281–288.
Jonas J, Rossion B, Krieg J, Koessler L, Colnat-Coulbois S, Vespignani H, Jacques C, Vignal J-P, Brissart H, Maillard L (2014): Intracerebral electrical stimulation of a face-selective area in the right inferior occipital cortex impairs individual face discrimination. Neuroimage 99:487–497.
Kilner JM, Kiebel SJ, Friston KJ (2005): Applications of random field theory to electrophysiology. Neurosci Lett 374:174–178.
Klopp J, Halgren E, Marinkovic K, Nenov V (1999): Face-selective spectral changes in the human fusiform gyrus. Clin Neurophysiol 110:676–682.
Lachaux, J. P., George N, Tallon-Baudry C, Martinerie J, Hugueville L, Minotti L, Kahane P, Renault B (2005): The many faces of the gamma band response to complex visual stimuli. Neuroimage 25:491–501.
Linkenkaer-Hansen K, Palva JM, Sams M, Hietanen JK, Aronen HJ, Ilmoniemi RJ (1998): Face-selective processing in human extrastriate cortex around 120 ms after stimulus onset revealed by magneto- and electroencephalography. Neurosci Lett 253:147–150.
Liu J, Harris A, Kanwisher N (2010): Perception of face parts and face configurations: an FMRI study. J Cogn Neurosci 22:203–211.
Mattout J, Henson RN, Friston KJ (2007) : Canonical source reconstruction for MEG. Comput Intell Neurosci 2007:67613.
Maurer D, Le Gand R, Mondloch CJ (2002): The many faces of configural processing. Trends Cogn Sci 6:255–260.
Meeren HKM, Hadjikhani N, Ahlfors SP, Hämäläinen MS, de Gelder B. (2008): Early category-specific cortical activation revealed by visual stimulus inversion. PLoS ONE 3: e3503.
Oldfield RC (1971): The assessment and analysis of handedness: the Edinburgh Inventory. Neuropsychologia 9:97–113.
Parvizi J, Jacques C, Foster BL, Witthoft N, Rangarajan V, Weiner KS, Grill-Spector K (2012): Electrical stimulation of human fusiform face-selective regions distorts face perception. J Neurosci 32:14915–14920.
Perry G, Singh KD (2014): Localizing evoked and induced responses to faces using magnetoencephalography. Eur J Neurosci 39:1517–1527.
Pitcher D, Walsh V, Duchaine B (2011): The role of the occipital face area in the cortical face perception network. Exp Brain Res 209:481–493.
Pitcher D, Walsh V, Yovel G, Duchaine B (2007): TMS evidence for the involvement

of the right occipital face area in early face processing. Curr Biol 17:1568–1573.
Pourtois G, Spinelli L, Seeck M, Vuilleumier P (2010): Modulation of face processing by emotional expression and gaze direction during intracranial recordings in right fusiform cortex. J Cogn Neurosci 22:2086–2107.
Prkachin GC (2003): The effects of orientation on detection and identification of facial expressions of emotion. Br J Psychol 94:45–62.
Purcell DG, Stewart AL (1986): The face-detection effect. Bull Psychon Soc. 24:118–120.
Pyles JA, Verstynen TD, Schneider W, Tarr MJ (2013): Explicating the face perception network with white matter connectivity. PLoS One 8:e61611.
Rakover SS (2012): A feature-inversion effect: can an isolated feature show behavior like the face-inversion effect? Psychon Bull Rev 19:617–624.
Ro T, Russell C, Lavie N (2001): Changing faces: a detection advantage in the flicker paradigm. Psychol Sci 12:94–99.
Rosburg T, Ludowig E, Dümpelmann M, Alba-Ferrara L, Urbach H, Elger CE (2010): The effect of face inversion on intracranial and scalp recordings of event-related potentials. Psychophysiology 47:147–157.
Rossion B (2008): Constraining the cortical face network by neuroimaging studies of acquired prosopagnosia. Neuroimage 40:423-426.
Rossion B, Caldara R, Seghier M, Schuller AM, Lazeyras F, Mayer E (2003): A network of occipito–temporal face-sensitive areas besides the right middle fusiform gyrus is necessary for normal face processing. Brain 126:2381–2395.
Rossion B, Jacques C (2008): Does physical interstimulus variance account for early electrophysiological face sensitive responses in the human brain? Ten lessons on the N170. Neuroimage 39:1959–1979.
Sadeh B, Podlipsky I, Zhdanov A, Yovel G (2010): Event-related potential and functional MRI measures of face-selectivity are highly correlated: a simultaneous ERP–fMRI investigation. Hum Brain Mapp 31:1490–1501.
Sato W, Kochiyama T, Uono S, Matsuda K, Usui K, Inoue Y, Toichi M (2013): Rapid and multiple-stage activation of the human amygdala for processing facial signals. Commun Integr Biol 6:e24562.
Sato W, Kochiyama T, Uono S, Matsuda K, Usui K, Inoue Y, Toichi M (2014): Rapid, high-frequency, and theta-coupled gamma oscillations in the inferior occipital gyrus during face processing. Cortex 60:52–58.
Schiltz C, Sorger B, Caldara R, Ahmed F, Mayer E, Goebel R, Rossion B (2006): Impaired face discrimination in acquired prosopagnosia is associated with abnormal response to individual faces in the right middle fusiform gyrus. Cereb Cortex 16:574–586.
Steeves JKE, Culham JC, Duchaine BC, Pratesi CC, Valyear KF, Schindler I, Humphrey GK, Milner AD, Goodale MA (2006): The fusiform face area is not sufficient for face recognition: evidence from a patient with dense prosopagnosia and no occipital face area. Neuropsychologia 44:594–609.
Tanaka JW (2001): The entry point of face recognition: Evidence for face expertise. J Exp Psychol Gen 130:534–543.
Tanskanen T, Näsänen R, Montez T, Päällysaho J, Hari R (2005): Face recognition and cortical responses show similar sensitivity to noise spatial frequency. Cereb Cortex 15:526–534.

Tong F, Nakayama K, Vaughan T, Kanwisher N (1998): Binocular rivalry and visual awareness in human extrastriate cortex. Neuron 21:753–759.

Tsuchiya N, Kawasaki H, Oya H, Howard MA III, Adolphs R (2008): Decoding face information in time, frequency and space from direct intracranial recordings of the human brain. PLoS ONE 3: e3892.

Uhlhaas, PJ, Pipa G, Neuenschwander S, Wibral M, Singer W. (2011): A new look at gamma? High- (>60 Hz) gamma-band activity in cortical networks: function, mechanisms and impairment. Prog Biophys Mol Biol 105:14–28.

van Veen BD, van Drongelen W, Yuchtman M, Suzuki A (1997): Localization of brain electrical activity via linearly constrained minimum variance spatial filtering. IEEE Trans Biomed Eng 44:867–880.

Vidal JR, Ossandón T, Jerbi K, Dalal SS, Minotti L, Ryvlin P, Kahane P, Lachaux JP (2010): Category-specific visual responses: An intracranial study comparing gamma, beta, alpha, and ERP response selectivity. Front Hum Neurosci 4:195.

Worsley KJ, Marrett S, Vandal NAC, Friston KJ, Evans AC (1996): A unified statistical approach for determining significant signals in images of cerebral activation. Hum Brain Mapp 4:58–73.

Yovel G, Kanwisher N (2005): The neural basis of the behavioral face-inversion effect. Curr Biol 15:2256-2262.

Zhao M, Cheung SH, Wong AC, Rhodes G, Chan EK, Chan WW, Hayward WG (2014): Processing of configural and componential information in face-selective cortical areas. Cogn Neurosci 5:160–167.

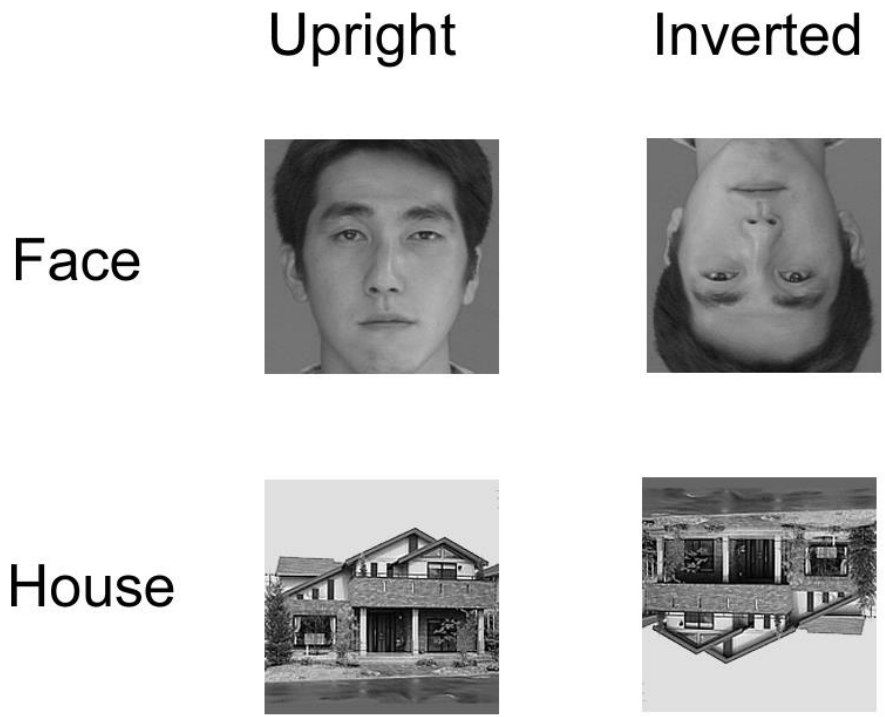

Figure 1. Examples of face and house stimuli.

Figure 2.

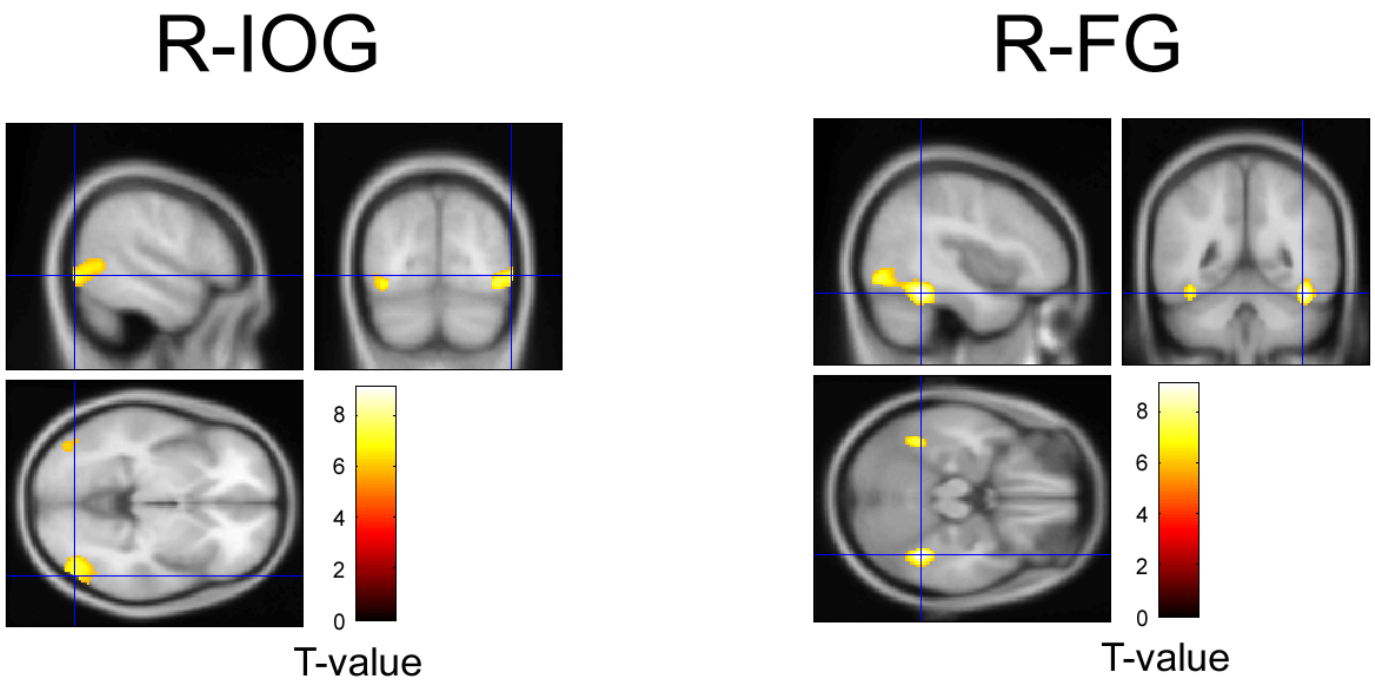

Figure 2. Statistical parametric map showing the activities in the IOG and FG for faces versus houses identified in a group analysis of fMRI data. R-: right.

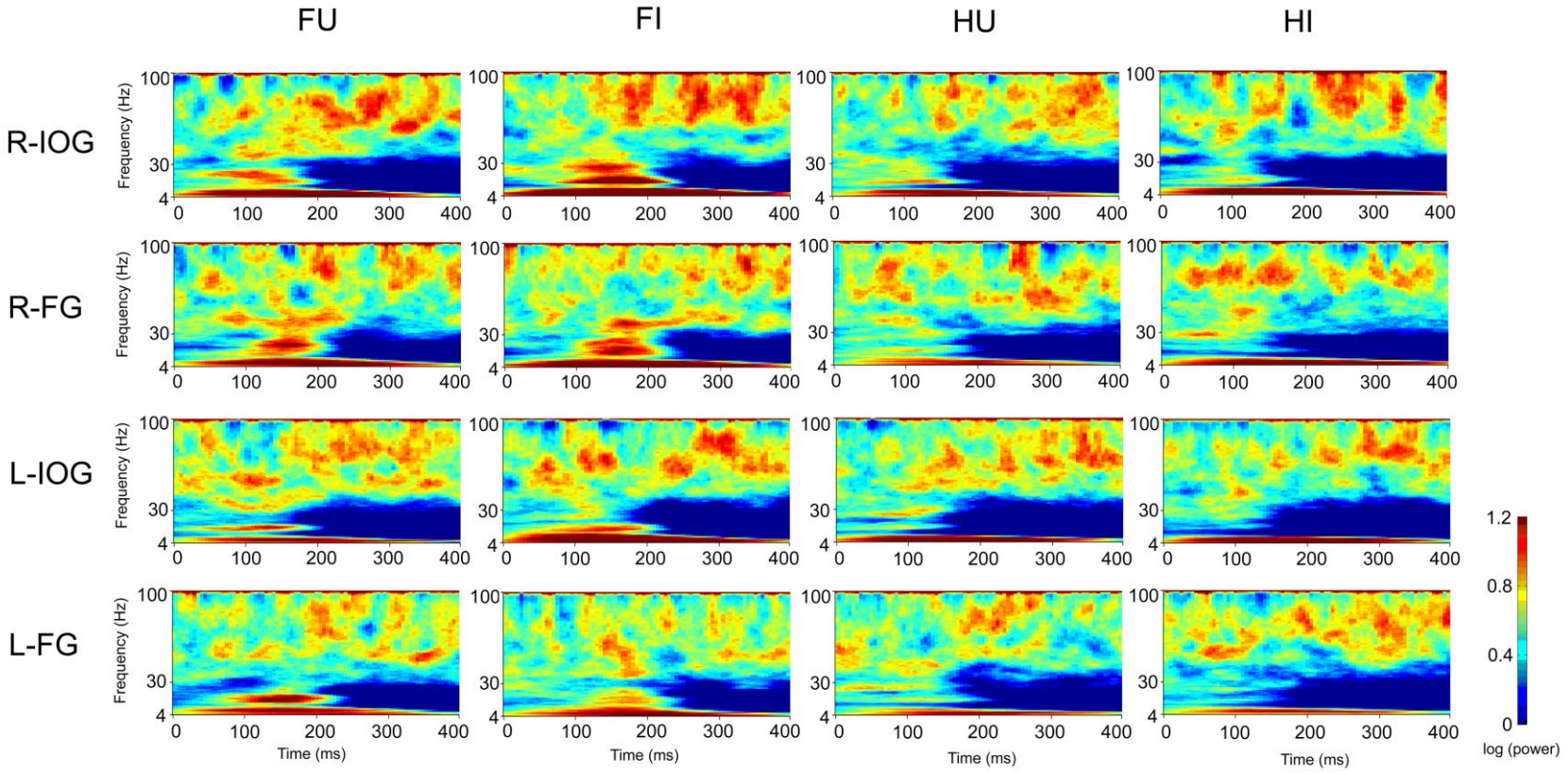

Figure 3. Time–frequency maps of bilateral IOG and FG activity. FU: upright face; FI: inverted face; HU: upright house; HI: inverted house; R-: right; L-: left.

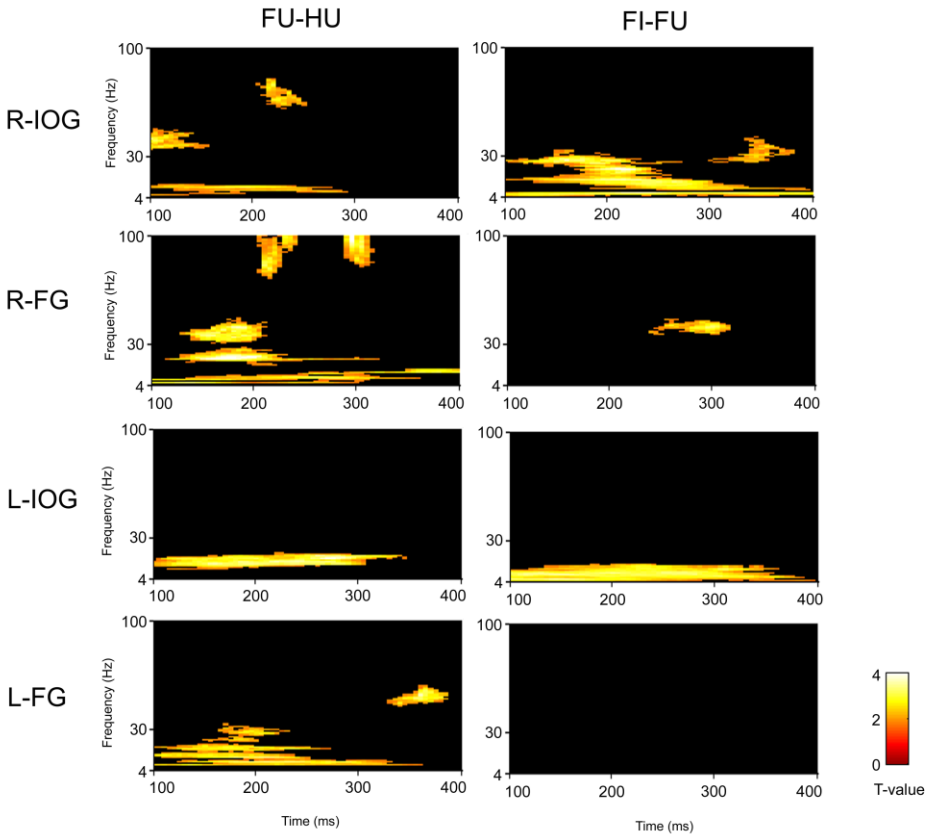

Figure 4. Statistical parametric maps for contrasts of the bilateral IOG and FG activity. FU: upright face; FI: inverted face; HU: upright house; R-: right; L-: left.

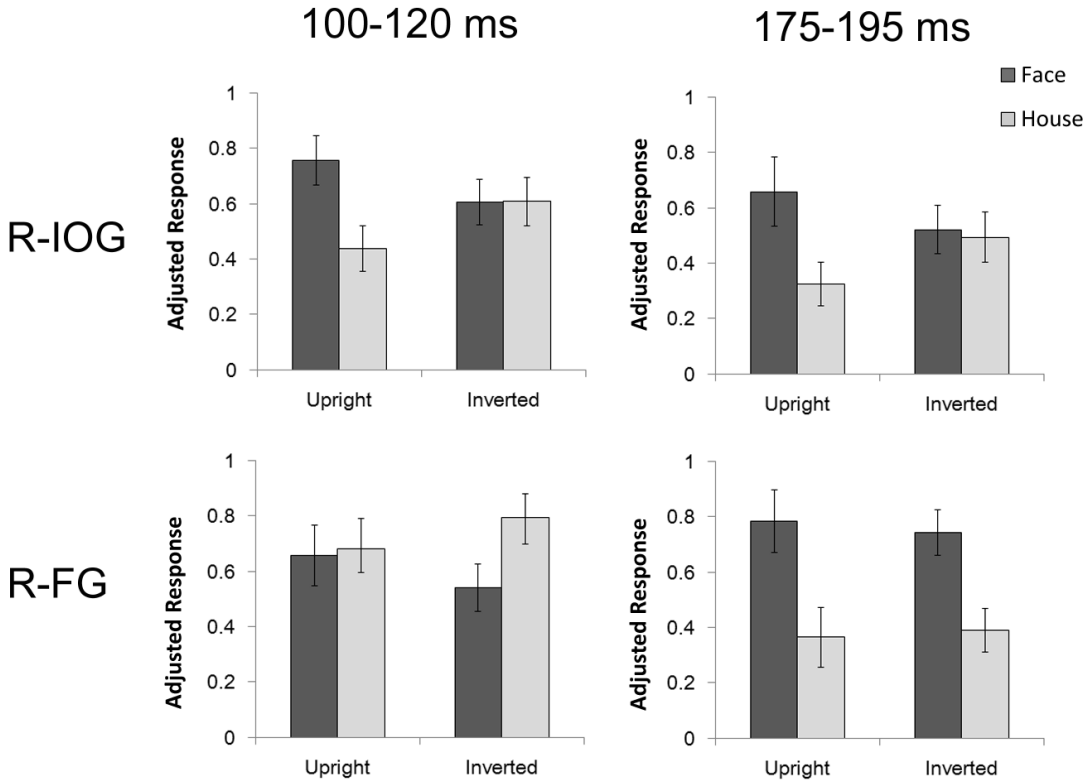

Figure 5. Normalized power of gamma-band activity in response to faces and houses in the right IOG and the FG. Time–frequency ranges (10 Hz, 20 ms) showing significant gamma-band activity in response to upright faces versus upright houses in the right IOG (36–46 Hz, 100–120 ms) and right FG (36–46 Hz, 175–195 ms) were the windows of interest. Error bars show the SE.

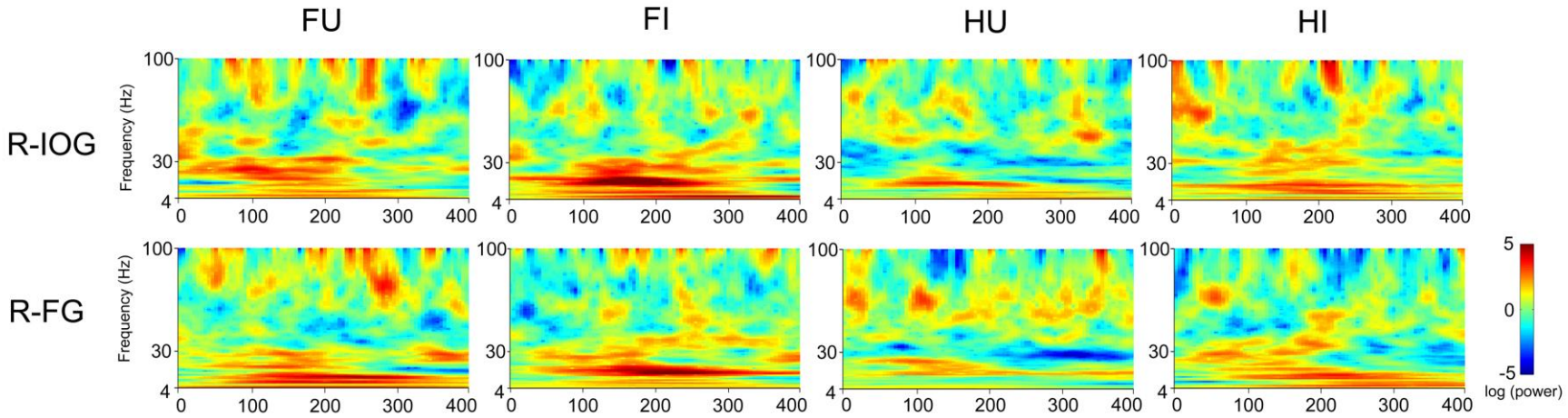

Supplementary Figure 1. Time–frequency maps of the evoked activity in the right IOG and FG.

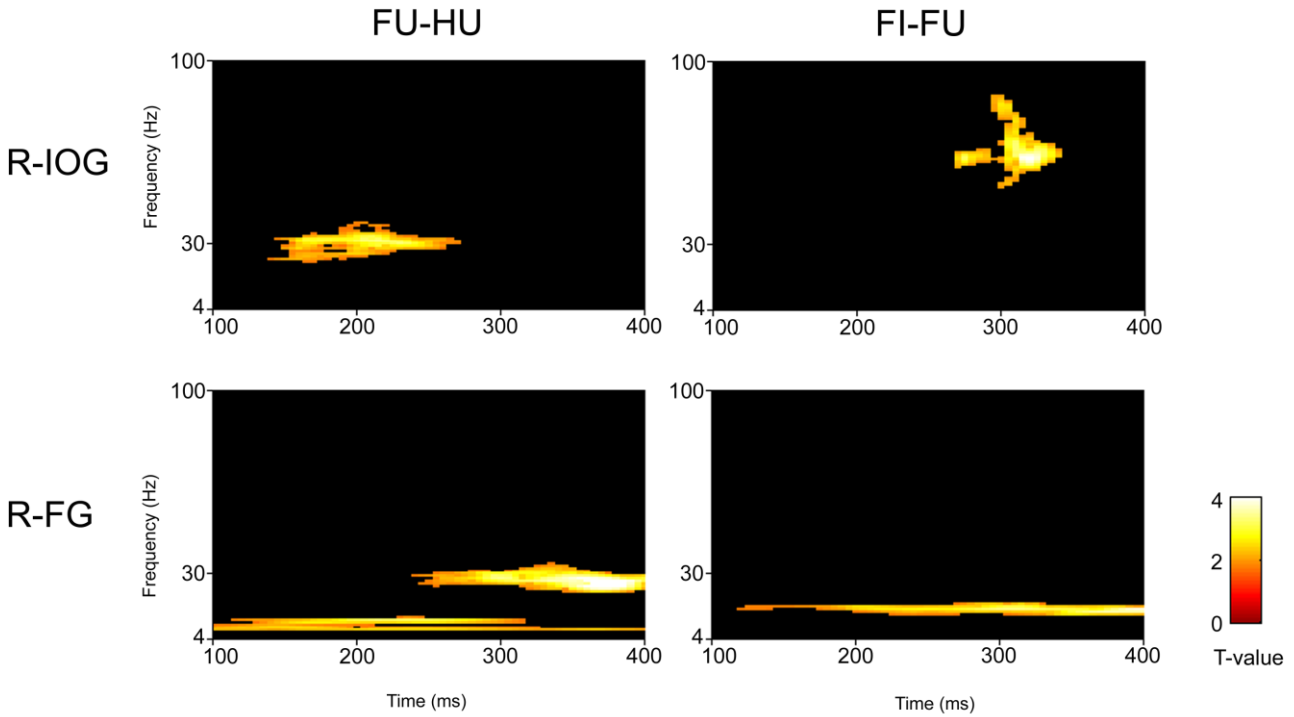

Supplementary Figure 2. Statistical parametric maps for contrasts of the right IOG and FG showing evoked activity.

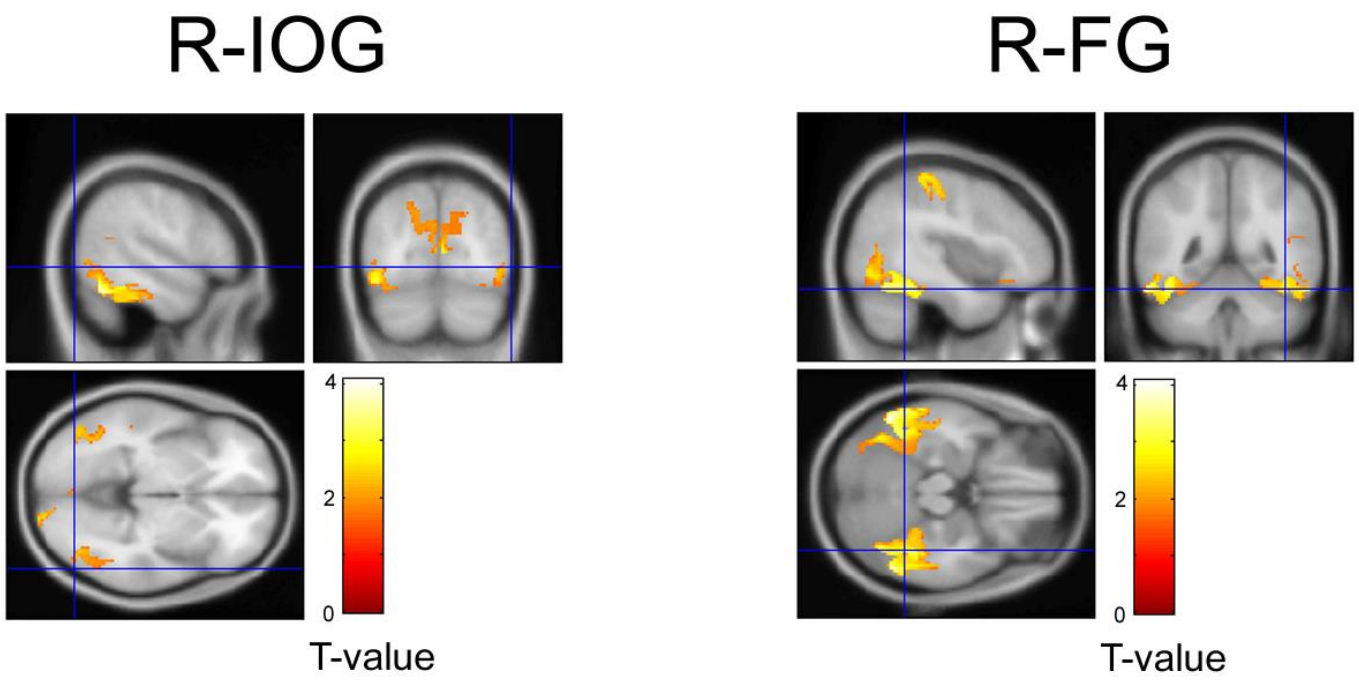

Supplementary Figure 3. Statistical parametric map of activity in the IOG and FG in response to upright faces versus upright houses identified by the source reconstruction analysis of MEG data.